Food Chemistry 151 (2014) 243–247

Contents lists available at ScienceDirect

Food Chemistry

journal homepage: www.elsevier.com/locate/foodchem

Colloidal iron(III) pyrophosphate particles

Laura Rossi [a,*], Krassimir P. Velikov [b,c,*], Albert P. Philipse [a]

[a] Van't Hoff Laboratory for Physical and Colloid Chemistry, Debye Institute for Nanomaterials Science, Utrecht University, Padualaan 8, 3584 CH Utrecht, The Netherlands
[b] Unilever R&D Vlaardingen, Olivier van Noortlaan 120, 3133 AT Vlaardingen, The Netherlands
[c] Soft Condensed Matter, Debye Institute for Nanomaterials Science, Utrecht University, Princetonplein 5, 3584 CC Utrecht, The Netherlands

ARTICLE INFO

Article history:
Received 30 May 2013
Received in revised form 30 October 2013
Accepted 11 November 2013
Available online 19 November 2013

Keywords:
Fortification
Ferric pyrophosphate
Colloidal particles

ABSTRACT

Ferric pyrophosphate is a widely used material in the area of mineral fortification but its synthesis and properties in colloidal form are largely unknown. In this article, we report on the synthesis and characterisation of colloidal iron(III) pyrophosphate particles with potential for application as a food additive in iron-fortified products. We present a convenient and food grade synthetic method yielding stable colloids of nanometre size with a distinctive white colour, a unique characteristic for iron-containing colloids. Physical properties of the colloids were investigated using different techniques, to assess particle crystallinity, surface charge, mass density, refractive index, internal structure, elemental composition and magnetic properties. The findings of this research are especially relevant for food and beverage science and technology and will help develop a more effective use of these fortifiers in colloidal form.

1.Introduction

The increasing knowledge of the relationship between food ingredients and their impact on human health is the origin of the growing demand for functional foods. Essential micronutrients, such as calcium, iron and zinc, just to mention a few, are not produced by the body and have to be introduced through a healthy and assorted diet or via food supplements. In particular, iron deficiency is very common, not only in developing countries, but also in industrialised countries and it is the main cause of anaemia (Zimmermann & Hurrell, 2007). In addition, consumers tend to prefer addressing common health problems such as mineral deficiency, obesity, diabetes, and cardiovascular health using food products rather than drugs (Diplock et al., 1999; Niva, 2007). The major issue is that delivery of iron in food products or supplements can be very problematic (Velikov & Pelan, 2008). Water-soluble iron salts (e.g. ferrous sulfate) are easily formulated and absorbed (good bioavailability), but often produce substantial changes in the colour and taste of foods. On the other hand, insoluble or poorly water-soluble compounds (e.g. ferric pyrophosphate), which generally cause less sensory change and are more stable in food, are not well absorbed (low bioavailability) (Hurrell, 2002).

Decreasing the size of insoluble iron-containing compounds, such as iron(III) pyrophosphate (ferric pyrophosphate, hereafter FePP) (Fidler et al., 2004) or iron phosphate (Hilty et al., 2010; Rohner et al., 2007) to nanoscale colloidal particles, can significantly increase the iron absorption without giving rise to organoleptic changes in the product (Velikov & Pelan, 2008). The high bioavailability and absorption of FePP nanoscale particles was demonstrated in rats and humans (Fidler et al., 2004; Wegmuller, Zimmermann, Moretti, & Arnold, 2004). Despite the wide use of ferric pyrophosphate, many of the basic properties of its colloidal form are not well established and only very recently insights into the colloidal stability and morphology of ferric pyrophosphate mixed salts were obtained (Van Leeuwen, Velikov, & Kegel, 2012a, 2012b, 2012c).

In this article we describe a study on the preparation of colloidal FePP particles of nanometre size, with a focus on characterisation of their physicochemical and material properties, as possible candidates for iron delivery systems.

2. Materials and methods

2.1. General procedure for particle preparation

Colloidal pyrophosphate particles were prepared using a straightforward precipitation reaction, (Van Leeuwen et al., 2012c) mixing sodium pyrophosphate decahydrate ($Na_4P_2O_7{\cdot}10H_2O$, $\geqslant$99%; Merck) and iron(III) chloride hexahydrate ($FeCl_3{\cdot}6H_2O$, ACS reagent 97%; Sigma–Aldrich) solutions. The net precipitation reaction is:

* Corresponding authors. Address: Department of Chemistry and Biochemistry, University of California–Los Angeles, Los Angeles, California 90095, USA. Tel.: +1 310 307 9040 (L. Rossi). Address: Unilever R&D Vlaardingen, Olivier van Noortlaan 120, 3133 AT Vlaardingen, The Netherlands. Tel.: +31 10 4605068 (K.P. velikov).
E-mail addresses: laura.rossi27@gmail.com (L. Rossi), krassimir.velikov@unilever.com (K.P. Velikov).

0308-8146/$ - see front matter © 2013 Elsevier Ltd. All rights reserved.
http://dx.doi.org/10.1016/j.foodchem.2013.11.050

$$4FeCl_3(aq) + 3Na_4P_2O_7(aq) \rightarrow Fe_4(P_2O_7)3(s) + 12NaCl(aq) \quad (1)$$

Reactions were performed at room temperature mixing stoichiometric ratios of reactants (4:3). In a typical reaction 20 mL of $FeCl_3$ (0.067 M) were dripped over 5 min via a separatory funnel into 70 mL of $Na_4P_2O_7$ (0.014 M) under magnetic stirring. To avoid hydrolysis of pyrophosphate anions to phosphate when stored in water (Hubner & Milburn, 1980), freshly prepared solutions in Millipore water were used for every synthesis.

2.2. Characterisation

2.2.1. Microscopy

Particle morphologies were studied by transmission electron microscopy (TEM, Philips TECNAI12) usually operating at 120 kV. Samples were prepared by drying drops of diluted particle dispersions on polymer-coated copper grids.

2.2.2. X-ray diffraction (XRD)

XRD measurements were performed on dried FePP colloids at room temperature on a Bruker-AXS D8 advance powder diffractometer, using Co $K\alpha_{1,2}$ radiation (λ = 1.79026 Å). The sample was prepared by drying a stable, concentrated aqueous dispersion of FePP particles in a glass vial. The powder obtained was used for the measurements.

2.2.3. Energy dispersive X-ray spectroscopy (EDX)

EDX analysis was performed using a scanning electron microscope (SEM, Philips XLFEG30) equipped with an EDX system (SEM-EDX). The measurements were performed on a thick particle sediment, which was prepared by drying a concentrated dispersion on a polymer-coated copper grid.

2.2.4. Zeta-potential

Zeta-potential (ζ-potential) measurements were performed on diluted aqueous dispersions of pyrophosphate colloids using a Malvern Zetasizer Nano NS at 25 °C.

2.2.5. Magnetisation measurements

Magnetisation curves were obtained using an alternating gradient magnetometer (MicroMag™ Model 2900 (AGM); Princeton Measurements Corp., Westerville, OH) operating at room temperature. Calibration was performed with an yttrium iron garnet sphere calibration sample purchased from the National Institute of Standards and Technology (NIST, Gaithersburg, MD). Measurements were performed on a small amount of powder obtained by drying an aqueous FePP dispersion as follows. The particles were dried on small (~3 × 3 mm) thin glass slides of known weight. After drying, the powder deposited on the glass piece was sealed using adhesive tape. The magnetic measurement was performed on the sealed sample; therefore a blank sample of glass and tape was measured in order to eliminate their contribution.

2.2.6. Mass density measurement

The mass density of pyrophosphate colloids ρ_p was determined by measuring the density of pyrophosphate dispersions ρ_d at different particle concentrations c, using the following relation:

$$\rho_d = \rho_s + c\left(1 - \frac{\rho_s}{\rho_p}\right) \quad (2)$$

where c is in expressed in mass per volume and ρ_s is the mass density of the solvent used, in this case water. The dispersion densities were measured using an Anton Paar density metre (DMA 5000; Anton Paar GmbH, Graz, Austria) at a constant temperature of T = 20.0 °C.

2.2.7. Refractive index measurement

An estimate of the refractive index value of pyrophosphate particles was made using the Avogadro–Biot-Beer–Landolt–Christiansen–Wintgen empirical formula (Heller, 1945) for volume-averaged refractive index:

$$n_t = \phi_w n_w + \phi_p n_p \quad (3)$$

where φ_w and φ_p are the volume fractions of the dispersant (water) and the particles; n_t, n_w and n_p are the refractive indices of the total dispersion, the dispersant (water) and the particles, respectively. The refractive index of each dispersion was measured using an Abbe refractometer (Carl Zeiss Jena) at λ = 589 nm (sodium D-line). Measurements were performed at room temperature (T = 20 °C).

3. Results and discussion

3.1. Particle preparation and stability

Fig. 1B shows a TEM image of a typical colloidal FePP prepared as described in Section 2, using stoichiometric ratios of iron and pyrophosphate ions (hereafter referred to as standard synthesis). The sample was dialysed using a Spectra/Por membrane (14,000 Daltons MWCO) against Millipore water for one week with daily replacement of the Millipore water reservoir. To preserve the particle stability, dialysis was performed only after one centrifugation step and dispersion of the sediments in water. The extra sedimentation step was introduced after experimental observations showed particle aggregation if dialysis was conducted immediately after precipitation. After dialysis we obtained a white stable dispersion which is shown in Fig. 1A.

The scenario drastically changed when the particles were precipitated using an excess of pyrophosphate. In this case, immediately after mixing the two starting solutions, only a small amount of sediment (compared to the standard synthesis) was formed, which disappeared after few minutes. This behaviour might be explained by the formation of soluble complexes which are known to form in the presence of excess pyrophosphate ions (Rogers & Reynolds, 1949). We assume that first the FePP precipitates and then quickly dissolves by complexation of the excess pyrophosphate ions present in solutions. We did not attempt to quantify the chemical composition of the transient sediment.

An important factor to consider when dealing with products intended as food supplements is their stability at different values of pH. To assess this stability, a batch of particles synthesised via the standard method was sedimented by centrifugation, the supernatant was removed and replaced with solutions with pH values from 2 to 10. The particles were stable in acidic solutions pH $\leqslant$ 7 and dissolved when dispersed in basic solutions above pH 7. The standard synthesis induced the formation of a stable dispersion

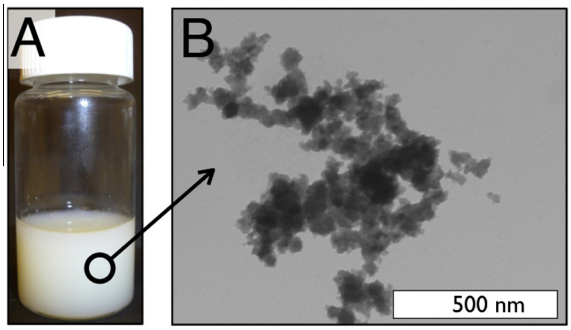

Fig. 1. Iron pyrophosphate colloids. (A) Iron pyrophosphate colloidal dispersion showing its typical milky-white colour when prepared with stoichiometric ratios of iron and pyrophosphate salts. (B) TEM image of particles prepared using stoichiometric ratio of reactants.

because the final pH of the dispersion was found to be around 5, which is a value that falls outside the pH range of dissolution.

The stability of the FePP dispersion is due to charges on the particle surface (Van Leeuwen et al., 2012b). The electrical mobility measurements performed on FePP aqueous dispersions purified by centrifugation and subsequent dialysis against Millipore water show a negative potential of about −50 mV. On the other hand, measurements on stable particles dispersed in acidic aqueous solutions (pH 2–3) gave a positive value of about +17 mV. An interesting aspect is that, while the particles changed the sign of the surface charges, hence passing through the point-of-zero-charge, no signs of flocculation were visible (Van Leeuwen et al., 2012b).

3.2. Particle characterization

The composition and internal structure of the FePP particles were investigated via SEM-EDX and XRD analysis. The SEM-EDX measurement was performed on a dried thick particle sediment, prepared as described in the Characterisation section. Due to the sample preparation technique the result yields an average value of elemental composition of the entire sediment. However, the data collected and showed in Fig. 2A clearly indicate the presence of oxygen, phosphorus and iron in the sample with element ratios that are very close to the theoretically calculated values based on the chemical formula $Fe_4(P_2O_7)_3$. Both measured and calculated values are listed in the table showed in Fig. 2A. The slight excess of oxygen atoms may be due to water molecules still present in the sample.

The internal particle structure was studied by powder-XRD analysis on dried particle sediments. As indicated by the lack of sharp peaks in the XRD diffraction data shown in Fig. 2B, the FePP colloids prepared with the method described in this chapter do not show any sign of internal crystalline structure, confirming that the particles are completely amorphous.

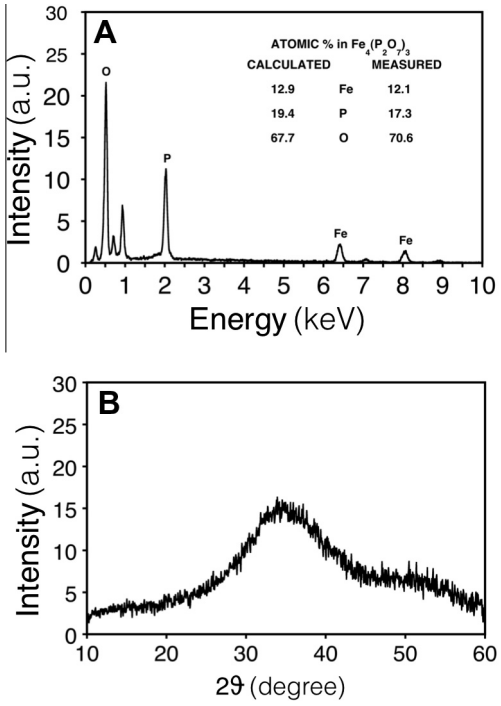

Fig. 2. Internal particle composition and structure. SEM-EDX (A) and powder-XRD (B) measurements performed on dried particle sediments. The average particle composition (A) indicates the presence of oxygen, phosphorus and iron in ratios similar to the calculated ones. The absence of sharp peaks in the XRD diffraction pattern of panel (B) is a sign of the amorphous nature of the FePP particles.

In order to better characterise the FePP colloids, density and refractive index measurements were performed. These two properties are very important when particles need to be formulated in liquid and/or transparent products, where sedimentation or turbidity may be an issue (Velikov & Pelan, 2008). For both measurements four stock dispersions with different particle weight concentrations were prepared (namely 2.09 %wt, 8.24 %wt, 9.91 %wt and 12.12 %wt). The densities of the stock dispersions are plotted in Fig. 3 against their product with the relative mass fractions. The points can be fitted with the linear equation $y = 0.63169x + 0.99818$, where 0.99818 g/cm^3 is the point of interception of the plotted line with the y-axis, and corresponds to the mass density of the solvent, in this case water. Equalising the experimental equation above with the theoretical one (Eq. (2)) we are left with the simple equation:

$$0.63169 = 1 - \left(\frac{\rho_{sol}}{\rho_p}\right) \tag{4}$$

which can be solved for ρ_p giving a particle density of 2.71 g cm^{-3}.

Due to interaction of solvent molecules with the surface of the colloids it is known that the relation between the particle concentration in dispersions and relative refractive indices is only linear for sufficiently low particle concentrations. To overcome this issue we have tried to apply the empirical formula shown in Eq. (3) for the four stock dispersions, with volume fractions calculated from the mass fractions using the dispersion and particle densities measured before. The values obtained for the different stock dispersions (listed from low to high mass fractions) are: 1.72, 1.61, 1.64, and 1.64. The values obtained are comparable, especially for the three most concentrated samples. To our knowledge this data represent the first estimate to date of the refractive index for colloidal FePP.

A very interesting aspect to be considered when working with iron-containing particles is their magnetic properties. The AGM measurement (Flanders, 1990) was performed on a small amount of dried FePP particles as described in the Characterisation section. Fig. 4A shows the measured magnetisation curves. All the curves pass from the axes origin (zero magnetisation) meaning that the material does not exhibit hysteresis, that is, there is no remanent magnetism in FePP. The black curve is a line with positive susceptibility, indicating that the magnetic field in the material is strengthened by the induced magnetisation, in which the intensity of magnetisation (M) is directly proportional to the intensity of the applied magnetic field (H), a behaviour typical of paramagnetic materials. (Hofmann, 2006) The blue curve of Fig. 4A is the black curve normalised for the diamagnetic contribution given by glass and tape; as a result the material shows a slightly higher susceptibility than the experimentally measured (non-normalised) value.

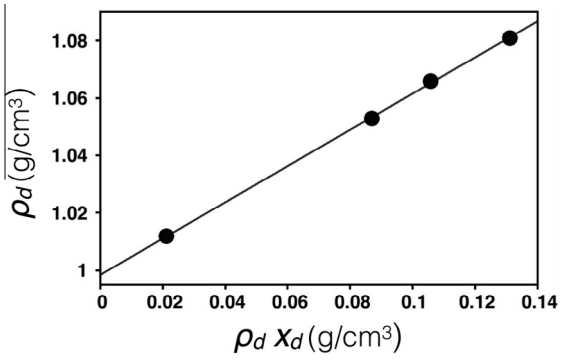

Fig. 3. Density measurement. The density of four dispersions with different particle concentrations is plotted against the product of the density and the mass fraction of the relative dispersions. The points are fitted with a straight line and the particle density is calculated using Eq. (2).

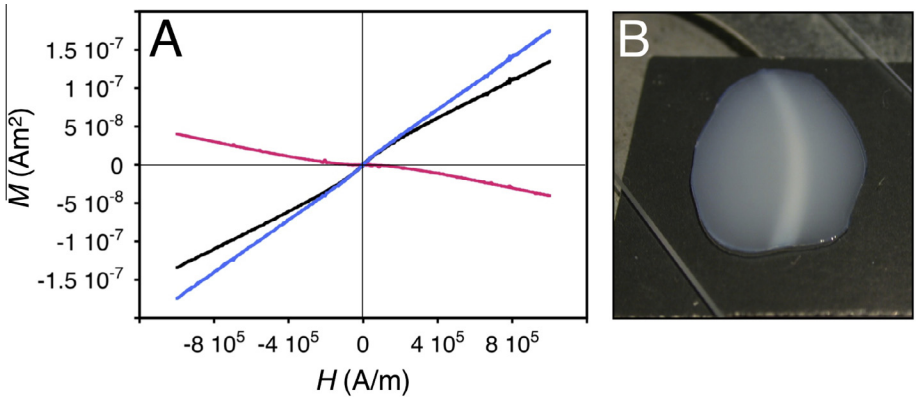

Fig. 4. Magnetic properties. (A) AGM magnetisation measurements on a dried sample of FePP colloids where the magnetisation (M) of the sample is plotted as a function of the applied magnetic field (H). The black curve is the FePP sample measured in a cell made of glass and adhesive tape. The pink curve represents the diamagnetic contribution of the sample cell and the blue curve was calculated subtracting the contribution of the sample cell (pink) to the FePP powder curve (black). The resulting black line shows no signs of remanent magnetisation and it is the typical curve of a paramagnetic material. Panel (B) shows that FePP particles sedimenting on top of a narrow magnet. The particles tend to collect and sediment in the central region where the highest field gradient is present. (For interpretation of the references to colour in this figure legend, the reader is referred to the web version of this article.)

An additional experimental observation of this paramagnetic effect can be seen in Fig. 4B in which a small amount of aqueous particle dispersion was placed on a glass microscope slide located on the surface of a thin circular magnet. As visible from the picture, most of the FePP colloids diffused towards the higher field line concentration in the centre of the magnetic section, showing that the FePP colloids are indeed magnetic. Although magnetic characterisation of ferrous pyrophosphates (Parada, Perles, Sáez-Puche, Ruiz-Valero, & Snejko, 2003), mixed ferrous-ferric pyrophosphates (Ijjaali, Venturini, Gerardin, Malaman, & Gleitzer, 1991; Malaman, Ijjaali, Gerardin, Venturini, & Gleitzer, 1992) and mixed ferric divalent metal pyrophosphates are available in the literature (Boonchom & Vittayakorn, 2010; Ramana, Kopec, Mauger, Gendron, & Julien, 2009; Terebilenko et al., 2010), so far we have not found magnetisation measurements and characterisation of amorphous ferric pyrophosphate. We hypothesise that the magnetic feature of FePP might be useful to detect its presence and avoid counterfeiting of iron-fortified products.

4. Conclusions

In this article we explore the preparation and characterisation of FePP colloidal particles. The particles are prepared via chemical precipitation from iron and pyrophosphate salts in an aqueous environment. The synthesis can only be performed from stoichiometric ratios of the reactants or an excess of iron ions. Using an excess of pyrophosphate induces the formation of water-soluble iron-pyrophosphate complexes (Rogers & Reynolds, 1949). To explore this colloidal system, basic charactersation experiments were carried out, such as X-ray diffraction and EDX, zeta potential, magnetisation, mass density and refractive index measurements. The nanoparticles obtained with this procedure are submicron in size (see Fig. 1B), white in colour and amorphous, all properties that indicate a high potential for FePP colloids as a food additive for iron-fortified products. Furthermore, the first characterisation of the magnetic properties of amorphous pyrophosphate opens the possibility for the preparation of white magnetic responsive materials and for control of FePP in fortified products.

Funding sources

We thank Agentschap NL of the Dutch Ministry of Economic Affairs for financial support; this work is financially supported by Food Nutrition Delta program grant FND07002.

Acknowledgements

Hans Meeldijk is thanked for performing SEM-EDX measurements and Marjan Versluijs-Helder (Inorganic Chemistry and Catalysis department) for performing XRD measurements. Dr. Ben Erné is thanked for his help with the magnetisation measurements. Prof. Willem Kegel and Dr. Mikal van Leeuwen are thanked for many useful discussions.

References

Boonchom, B., & Vittayakorn, N. (2010). Synthesis and ferromagnetic property of new binary copper iron pyrophosphate $CuFeP_2O_7$. *Materials Letters, 64*(3), 275–277. http://dx.doi.org/10.1016/j.matlet.2009.10.058.

Diplock, A. T., Aggett, P. J., Ashwell, M., Bornet, F., Fern, E. B., & Roberfroid, M. B. (1999). Scientific concepts in functional foods in Europe: Consensus document. *British Journal of Nutrition, 81*.

Fidler, M. C., Walczyk, T., Davidsson, L., Zeder, C., Sakaguchi, N., Juneja, L. R., et al. (2004). A micronised, dispersible ferric pyrophosphate with high relative bioavailability in man. *British Journal of Nutrition, 91*, 107–112. http://dx.doi.org/10.1079/BJN20041018.

Flanders, P. J. (1990). A vertical force alternating gradient magnetometer. *Review of Scientific Instruments, 61*(2), 839–847.

Heller, W. (1945). The determination of refractive indices of colloidal particles by means of a new mixture rule or from measurements of light scattering. *Physical Review, 68*, 5–10.

Hilty, F. M., Arnold, M., Hilbe, M., Teleki, A., Knijnenburg, J. T. N., Ehrensperger, F., et al. (2010). Iron from nanocompounds containing iron and zinc is highly bioavailable in rats without tissue accumulation. *Nature Nanotechnology, 5*(5), 374–380. http://dx.doi.org/10.1038/NNANO.2010.79.

Hofmann, P. (2006). *Solid state physics*. Weinheim: Wiley-VCH.

Hubner, P. W. A., & Milburn, R. M. (1980). Hydrolysis of pyrophosphate to orthophosphate promoted by cobalt(III). Evidence for the role of polynuclear species. *Inorganic Chemistry, 19*, 1267–1272.

Hurrell, R. (2002). Fortification: Overcoming technical and practical barriers. *Journal of Nutrition, 132*(4), 806S–812S.

Ijjaali, M., Venturini, G., Gerardin, R., Malaman, B., & Gleitzer, C. (1991). Synthesis, structure and physical-properties of a mixed-valence iron diphosphate $Fe_3(P_2)7)_2$ – 1st Example of trigonal prismatic Fe^{2+} with O^{2-} ligands. *European Journal of Solid State and Inorganic Chemistry, 28*, 983.

Malaman, B., Ijjaali, M., Gerardin, R., Venturini, G., & Gleitzer, C. (1992). $Fe_7(P_2O_7)_4$, a mixed-valence iron diphosphate, the missing link between $Fe_2P_2O_7$ and $Fe_3(P_2O_7)_2$. *European Journal of Solid State and Inorganic Chemistry, 29*, 1269.

Niva, M. (2007). "All foods affect health": Understandings of functional foods and healthy eating among health-oriented Finns. *Appetite, 48*(3), 384–393. http://dx.doi.org/10.1016/j.appet.2006.10.006.

Parada, C., Perles, J., Sáez-Puche, R., Ruiz-Valero, C., & Snejko, N. (2003). Crystal growth, structure, and magnetic properties of a new polymorph of $Fe_2P_2O_7$. *Chemistry of Materials, 15*(17), 3347–3351. http://dx.doi.org/10.1021/cm034137a.

Ramana, C. V., Kopec, M., Mauger, A., Gendron, F., & Julien, C. M. (2009). Structure and magnetic properties of nanophase-$LiFe_{1.5}P_2O_7$. *Journal of Applied Physics, 106*(6), 064304. http://dx.doi.org/10.1063/1.3213093.

Rogers, L., & Reynolds, C. (1949). Interaction of pyrophosphate ion with certain multivalent cations in aqueous solutions. *Journal of the American Chemical Society, 71*(6), 2081–2085.

Rohner, F., Ernst, F. O., Arnold, M., Hibe, M., Biebinger, R., Ehrensperger, F., et al. (2007). Synthesis, characterization, and bioavailability in rats of ferric phosphate nanoparticles. *Journal of Nutrition, 137*(3), 614–619.

Terebilenko, K. V., Kirichok, A. A., Baumer, V. N., Sereduk, M., Slobodyanik, N. S., & Guetlich, P. (2010). Structure and magnetic properties of $AgFeP_2O_7$. *Journal of Solid State Chemistry, 183*(6), 1473–1476. http://dx.doi.org/10.1016/j.jssc.2010.03.042.

Van Leeuwen, Y. M., Velikov, K. P., & Kegel, W. K. (2012a). Morphology of colloidal metal pyrophosphate salts. *RSC Advances, 2*(6), 2534. http://dx.doi.org/10.1039/c2ra00449f.

Van Leeuwen, Y. M., Velikov, K. P., & Kegel, W. K. (2012b). Repeptization by dissolution in a colloidal system of iron(III) pyrophosphate. *Langmuir, 28*(48), 16531–16535. http://dx.doi.org/10.1021/la303668a.

Van Leeuwen, Y. M., Velikov, K. P., & Kegel, W. K. (2012c). Stabilization through precipitation in a system of colloidal iron(III) pyrophosphate salts. *Journal of Colloid and Interface Science, 381*(1), 43–47. http://dx.doi.org/10.1016/j.jcis.2012.05.018.

Velikov, K. P., & Pelan, E. (2008). Colloidal delivery systems for micronutrients and nutraceuticals. *Soft Matter, 4*(10), 1964. http://dx.doi.org/10.1039/b804863k.

Wegmuller, R., Zimmermann, M., Moretti, D., & Arnold, M. (2004). Particle size reduction and encapsulation affect the bioavailability of ferric pyrophosphate in rats. *Journal of Nutrition, 134*(12), 3301–3304.

Zimmermann, M. B., & Hurrell, R. F. (2007). Nutritional iron deficiency. *Lancet, 370*(9586), 511–520.